A Portable Gait Monitoring System for Lower Limb Prosthetic Alignment

Kian Sek Tee, *Member, IAENG*, Mohammed Awad, Abbas Dehghani, David Moser and Saeed Zahedi

***Abstract*— Lower limb prosthetic alignment is time consuming and subjective, i.e. dependant to the experience of the prosthetists and feedbacks from the amputees. Alignment settings differ from one prosthetist to another. On the other hand, researchers believe that there is an optimum alignment for each amputee. Proper alignment is vital to provide sufficient gait function and comfort. Instrumental gait analysis is crucial to provide scientific data about the effect of alignment. However, commercial gait monitoring systems are expensive. To assess the effect of alignment, the author demonstrates the design and development of a low-cost gait measurement system to acquire kinematic information using inertial measurement units (IMUs). A heuristic approach to interpret IMU outputs during motion was proposed. Feasibility test of the system showed that critical gait events such as Heel Contact (HC) and Push-Off (PO) could be identified.**

***Index Terms*—** gait analysis, alignment, IMU, lower limb prosthesis.

I. Introduction

Lower limb prosthesis alignment [1, 2] is vital to provide comfort in the stump-socket interface and will affect the gait function of the amputees. Researchers [1-9] had looked into the alignment issues of lower limb prosthesis for decades and a number of gait performance indicators such as symmetry [3], balance [5], roll-over-shape [9], etc., were suggested. However, none of those techniques could confidently indicate and lead to the theoretical optimum alignment setup. Zahedi [2] had defined several key alignment parameters but discovered that the amputees could accept a broad range of setup due to adaptations. Sin [10] showed that non-level walking could restrict the range of accepted setup. Temporal-spatial [1, 3, 9] , kinetic [1, 5, 7, 8], kinematic [1, 4] and energy consumption [11] information are used by researchers to provide an objective gait assessment.

A reliable gait measurement system is needed to justify the gait quality. Commercial gait measurement devices such as force plate, motion capture camera, etc, are expensive and non-portable. Gait measurement using automotive standard accelerometers and gyroscopes are popular nowadays because they are cheap, consistent and reliable. Thus, the author has developed a customized portable gait monitoring system using IMUs to acquire kinematic information of the body segments. This paper illustrates the design and the development of the system, followed by a gait study of the system onto a healthy subject.

Kian Sek Tee, Mohammed Awad, Abbas Dehghani are with the Institute of Engineering Systems and Design (iESD), University of Leeds, LS2 9JT, United Kingdom. (Phone: 0113 343 2186; Fax: 0113 242 4611; e-mail: mnkst@ leeds.ac.uk). Kian Sek Tee is also an academic staff of University Tun Hussein Onn Malaysia, Parit Raja, Batu Pahat, 86400, Johor, Malaysia.

David Moser and Saeed Zahedi are with Chas A Blatchford & Sons Ltd, Lister Road, Basingstoke, Hampshire, RG22 4AH, United Kingdom.

II. System

The portable gait monitoring system consists of a battery powered data logger, five units of IMU-5DOF, Velcro straps and carriers as shown in Fig.1.

(a) (b)

Fig.1: (a) Data Logger and carrier, (b) IMU and bracket

A. Datalogger

The data logger is battery-powered, light and portable. It has 32 analog inputs channels which acquire up to 3.3V at 200Hz sampling rate, a 2 x 16 LCD display, 1GB storage using a Secure Digital (SD) card and a push button to trigger the data logging events. The core processor is based on Mbed microcontroller, NXP LPC1768. Via Serial Peripheral Interface (SPI), four units of MCP3008 10-bit Analog-to-Digital Converter (ADC) and a SD card were used to construct 32 analog inputs and 1GB data storage respectively. All analog channels were calibrated by varying input voltage from 0V to 3.3V at 0.1V interval for approximately 10 second each sample. An example of the digital-analog relationship between mean digital number and voltages is shown as Fig.2. Maximum standard error (SE) of the binary numbers at 1.05 was observed, which means for 95% confidence interval, voltage measurement error would fluctuate around 6.7mV. Equation (1) represents the digital-to-analog (DAC) relationship between the measured voltage (V) and corresponding digital number (N). This is used for digital-to-analog convertion.

$$\boldsymbol{V} = \frac{\boldsymbol{N} \times \boldsymbol{3.3}}{\boldsymbol{1024}} \ (\boldsymbol{V}) \qquad (1)$$

ISBN: 978-988-19251-5-2
ISSN: 2078-0958 (Print); ISSN: 2078-0966 (Online)

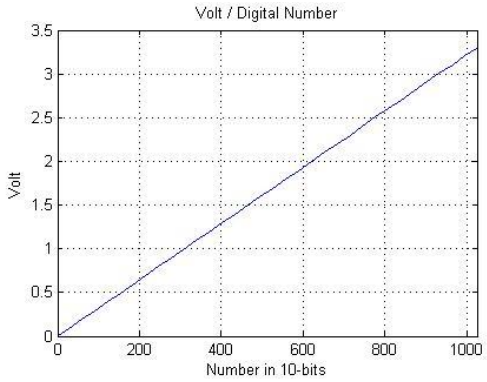

Fig.2: Digital to Analog

B. IMU and Calibration

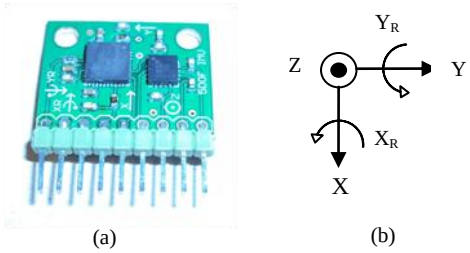

(a) (b)

Fig.3: (a) IMU-5DOF, (b) Axes assignment

An IMU-5DOF in the form of a PCB breakout (SparkFun Inc.) such as shown in Fig.3a was used. It consists of a triaxial (X,Y,Z) accelerometer (ADXL330, Analog Device) and a dual axial (X_R,Y_R) gyroscope (IDG300, InvenSense Inc). The axes assignment (Fig.3b) follows the recommendation of ADXL330 datasheet. The direction of axes assignment follows the norm that the accelerometer axis points upward against the gravity and gyroscope turning direction is positive as labelled. Accelerometer is ratiometric, that means zero bias and scale factor varies relative to the input voltage change. Nevertheless, gyroscope is non-ratiometric.

All IMU-5DOF were statically calibrated by positioning the unit in six orientations where each accelerometer axis experienced ±1g. A triaxial accelerometer and a dual-axis gyroscope are modelled as (2) and (3) respectively. Scale factor of the gyroscope is given by the manufacturer as *2mV/ ^{0}/s* and is identical for both axes (k_{gx}, k_{gy}). Calibration is needed to experimentally acquire the scale factors and zero bias for both accelerometer and gyroscope as listed in (4).

$$\boldsymbol{V_{ai}} = \boldsymbol{K_a s_i} + \boldsymbol{b_a} \tag{2}$$

$$\boldsymbol{V_{gi}} = \boldsymbol{K_g \omega_i} + \boldsymbol{b_g} \tag{3}$$

where:

$\boldsymbol{V_{ai}}$ *Accelerometer output vector* $[v_{ax}\ v_{ay}\ v_{az}]^T$ *at i-sample in volts*

$\boldsymbol{K_a}$ *Diagonal matrix of accelerometer scale factors. Diag(*$[k_{ax}\ k_{ay}\ k_{az}]$*) in volts/g*

$\boldsymbol{s_i}$ *g-force vector in each axis* $[g_x\ g_y\ g_z]^T$ *at i-sample*

$\boldsymbol{b_a}$ *Accelerometer zero bias vector of each axis.* $[b_{ax}\ b_{ay}\ b_{az}]^T$ *in volts*

$\boldsymbol{V_{gi}}$ *Gyroscope output vector* $[v_{gx}\ v_{gy}]^T$ *at i-sample in volts*

$\boldsymbol{K_g}$ *Diagonal matrix of gyroscope scale factors. Diag(*$[k_{gx}\ k_{gy}]$*) in volts/degree/second.*

$\boldsymbol{\omega_i}$ *angular speed in each axis* $[w_x\ w_y]^T$ *at i-sample*

$\boldsymbol{b_g}$ *Gyroscoope zero bias vector of each axis.* $[b_{gx}\ b_{gy}]^T$ *in volts*

$$\begin{bmatrix} k_{ax} & k_{ay} & k_{az} & b_{ax} & b_{ay} & b_{az} & b_{gx} & b_{gy} \end{bmatrix} \tag{4}$$

C. Body Landmarks and Axis Assignment

IMUs were positioned at lateral thighs and lateral shanks as well as at body centre of mass (BCoM), using Velcro straps as shown in Fig. 4. All IMU are mounted on Perspex cubes.

Local coordinates adopted IMU axes assignment. During quite stance, for the limb segments, X-axis is pointing laterally; Y-axis is pointing anteriorly and Z-axis is pointing upward against the gravity. Meanwhile, at BCOM, IMU is arranged in a different way, i.e. X-axis is pointing upward against the gravity; Y-axis is pointing laterally and Z-axis is pointing posteriorly. Since IMUs at both legs are mirror to each other, (X, Y) and (X_R, Y_R) are inverse in directions. For comparison purposes, kinematic readings at the left side were inversed to match the right side.

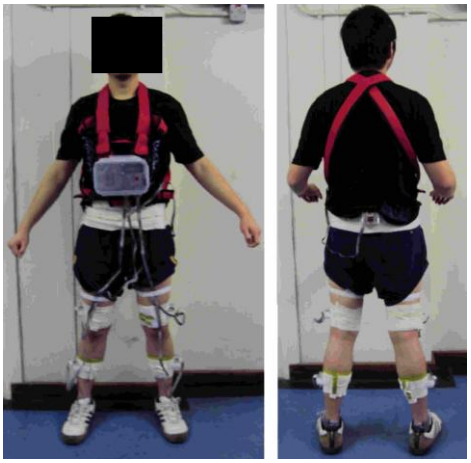

Fig. 4: Body landmarks and IMU axes assignments

D. Heuristic Interpretation of IMU Kinematic Data

The author proposed two experiment setups to heuristically interpret an IMU outputs during motions. Firstly a compound pendulum (Fig. 5a) was designed to mimic a leg motion. Secondly a free-drop test (Fig. 6) was performed to mimic heel contact. An IMU oriented in Y-Z plane was mounted in both setup. As illustrated in Fig. 5b, Y-axis reads the tangential acceleration; Z-axis reads the radial acceleration and X_R-axis reads the angular speed. To interpret kinematic data during swing phase, the pendulum was released repetitively from the left or the right side in separate trials. A sample of IMU outputs released from the right side is illustrated in Fig. 7. A number of outputs features were observed. Firstly, the radial acceleration (Z-axis) was obviously larger than the tangential acceleration (Y-axis). Secondly, the radial acceleration was positive while the

ISBN: 978-988-19251-5-2
ISSN: 2078-0958 (Print); ISSN: 2078-0966 (Online)

tangential acceleration fluctuated at near zero g. Gyroscope signs, i.e. clockwise or anti-clockwise could be determined. Meanwhile, to heuristically interpret the IMU responses upon acute speed changes such as heel contact (HC) and push-off (PO), the pendulum was gently tap at the left side and right side repetitively during swings. Fig.8 illustrates IMU outputs in Y-Z planes while tapping gently at the right side. Acute and short spikes were observed at the tangential acceleration. Tapping at the right side results in negative spike while tapping at the left side results in positive spike. An example of the result of a free-drop test in Y-Z plane was illustrated in Fig. 9, where Y-axis was horizontal to the right and Z-axis was vertically upward. Immediate decrement in g-acceleration in the vertical axis was observed at free drop, followed by a positive spike at impact but both the horizontal axis and angular speed did not exhibit obvious rhythmic changes during the event of free drop.

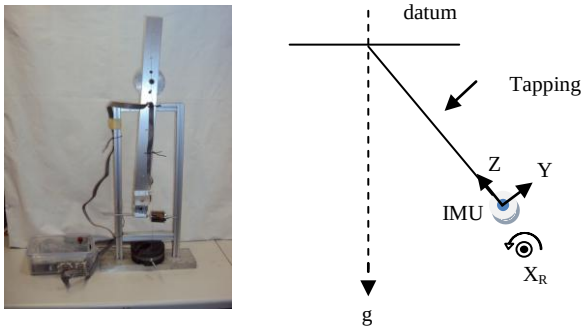

(a). Pendulum (b). Right to Left

Fig. 5: (a). Pendulum rig, (b). Right to Left

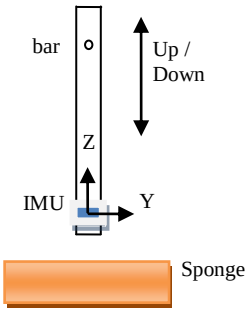

Fig. 6: Free-drop test

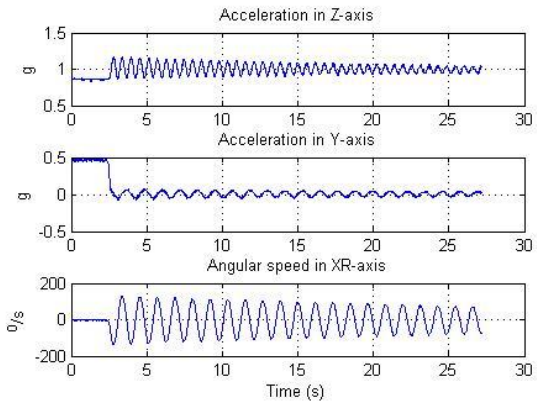

Fig. 7: Y,Z and X_R-axis responses when release from the right side

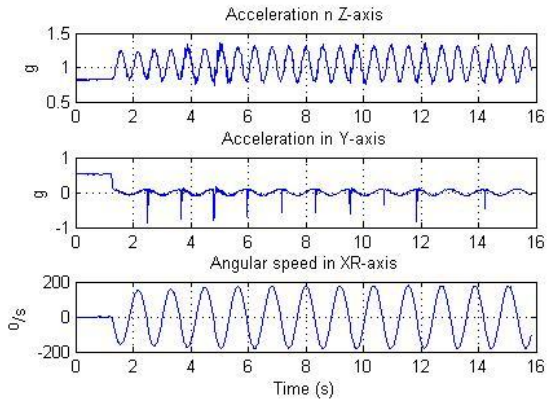

Fig.8: Y,Z and X_R-axis responses when tapping at the right side

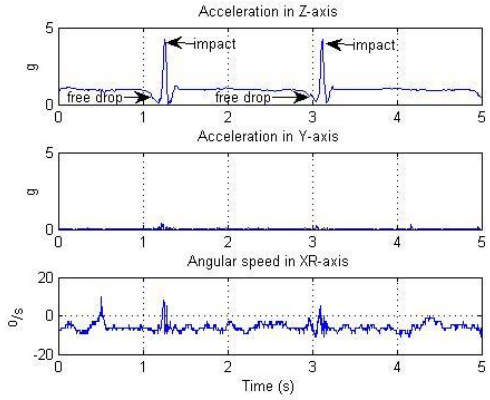

Fig. 9: Y, Z and X_R-axis responses during a free-drop test

III. Gait Measurement

A gait study of the portable gait monitoring system was performed. Gait data of a healthy subject at normal walking speed were collected. Several gait features were interpreted and identified. Some of the features are illustrated here. All gait data were post-processed using Matlab.

An example of the measured gait data at the right shank is illustrated in Fig. 10. The IMU displayed repetitive gait patterns especially at (X, Y, Z) and (X_R, Y_R) axis. Accelerometer outputs (X, Y and Z) were not normalized but in actual acceleration in unit of g. Results in lateral plane are much significant than other planes. A positive spike (Z-axis) followed by a transient was observed during heel contact (HC) and at the same time, lateral angular speed (X_R) was near zero, indicating the beginning of stance phase (St). Both Z-axis and Y-axis stabilized with little excursion in X_R axis at stance (St). At push-off (PO), significant positive increasing in Z and Y axis were observed, indicating the beginning of swing (Sw). The swing phase (Sw) was easily seen as the biggest excursion of the angular speed. A smaller spike toward zero in the angular speed (X_R) was observed during heel contact. Similar gait patterns from IMU data was reported by Lai [12]. Significant signal pattern changes were observed at IMU at distal positions but experienced attenuation at proximal positions. These findings agreed with Kavanagh [13].

ISBN: 978-988-19251-5-2
ISSN: 2078-0958 (Print); ISSN: 2078-0966 (Online)

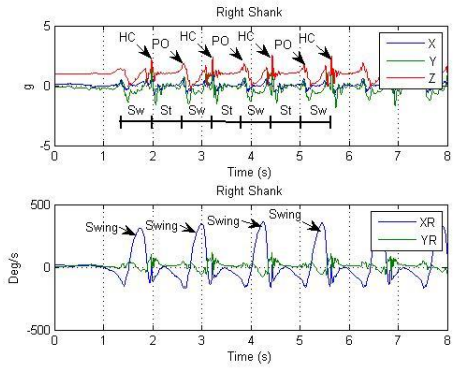

Fig. 10: Gait events identification

A comparison of accelerations of right and right shanks are illustrated in Fig. 11. Left leg shows very similar gait patterns as the right leg but at offset phases. Double stance occurs at the moment of right heel contact (HC) and left push off (PO).

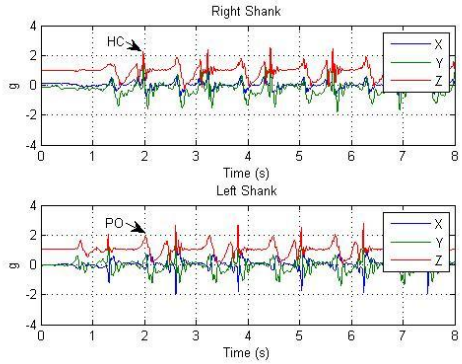

Fig. 11: Right and Left leg gait events identifications

A check on X-axis of BCoM reveals the step information. Unprocessed signal is too noisy due to vibration, however step information could be roughly read. The signal was filtered with a Butterworth low pass filter, designed at 1.5Hz cut-off frequency. Step information was clearer after filtering. A window smoothing algorithm was performed to smooth out small ripples along the peaks and valleys. Finally, steps were counted from the number of peaks. Meanwhile, mean step (0.61s) and its standard deviation (0.10s) could be calculated from reorganized time array of each peaks.

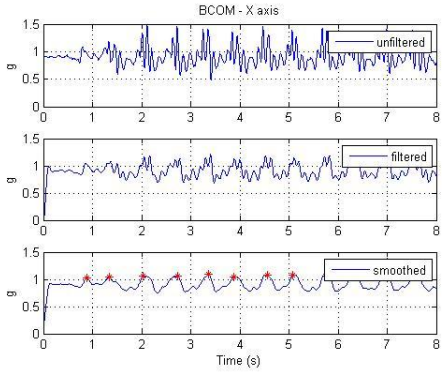

Fig. 12: X axis of BCOM

IV. Conclusion

Design and development of a customized portable gait monitoring system to assess prosthesis alignment was demonstrated. Data logger and IMUs were carefully calibrated. Important body landmarks and IMU axes assignment were recommended and applied throughout the design. Furthermore, the author had introduced two experiment setups to heuristically interpret an IMU's outputs. The system was trialed and the critical gait events were identified. Repetitive data patterns suggest that the system could be used to measure gait. Cumulative gait features may be used for statistical comparison. Future efforts include analyzing and assessing gait efficiencies in temporal or kinematic parameters under the changes of prosthesis alignments.

References

[1] L. Yang, S. E. Solomonidis, and J. P. Paul, "The influence of limb alignment on the gait of above-knee amputees," *Journal of Biomechanics*, vol. 24, pp. 981-997, 1991.

[2] M. S. Zahedi, W. D. Spence, S. E. Solomonidis, and J. P. Paul, "Alignment of lower-limb prostheses," *J Rehabil Res Dev.*, vol. 23, pp. 2-19, 1986.

[3] R. E. Hannah, J. B. Morrison, and A. E. Chapman, "Prostheses alignment: effect on gait of persons with below-knee amputations," *Arch Phys Med Rehabil*, vol. 65, pp. 159-162, 1984.

[4] G. Kerr, M. Saleh, and M. O. Jarrett, "An angular alignment protractor for use in the alignment of below-knee prostheses " *Prosthetics and Orthotics International*, vol. 8, pp. 56-57, 1984.

[5] E. Isakov, J. Mizrahi, Z. Susak, I. Ona, and N. Hakim, "Influence of prosthesis alignment on the standing balance of below-knee amputees," *Clinical Biomechanics*, vol. 9, pp. 258-262, 1994.

[6] S. W. Sin, D. H. K. Chow, and J. C. Y. Cheng, "A new alignment jig for quantification and prescription of three-dimensional alignment for the patellar-tendon-bearing trans-tibial prosthesis," *Prosthetics and Orthotics International*, vol. 23, pp. 225-230, 1999.

[7] S. Blumentritt, "A new biomechanical method for determination of static prosthetic alignment," *The Journal of the International Society for Prosthetics and Orthotics*, vol. 21, pp. 107-113, 1997.

[8] J. W. Breakey, "Theory of Integrated Balance: The Lower Limb Amputee," *Journal of Prosthetics & Orthotics*, vol. 10, pp. 42-44, 1998.

[9] A. H. Hansen, M. R. Meier, M. Sam, D. S. Childress, and M. L. Edwards, "Alignment of trans-tibial prostheses based on roll-over shape principles," *Prosthetics and Orthotics International*, vol. 27, pp. 89-99, 2003.

[10] S. W. Sin, D. H. Chow, and J. C. Cheng, "Significance of non-level walking on transtibial prosthesis fitting with particular reference to the effects of anterior-posterior alignment," *J Rehabil Res Dev*, vol. 38, pp. 1-6, 2001.

[11] T. Schmalz, S. Blumentritta, and R. Jaraschb, "Energy expenditure and biomechanical characteristics of lower limb amputee gait: The influence of prosthetic alignment and different prosthetic components " *Gait & Posture*, vol. 16, pp. 255 - 263 2002.

[12] D. T. H. Lai, R. Begg, E. Charry, and M. Palaniswami, "Frequency analysis of inertial sensor data for measuring toe clearance," *Intelligent Sensors, Sensor Networks and Information Processing, 2008. ISSNIP 2008. International Conference on*, pp. 303-308, 2008.

[13] J. J. Kavanagh and H. B. Menz, "Accelerometry: A technique for quantifying movement patterns during walking," *Gait & Posture*, vol. 28, pp. 1-15, 2008.

ISBN: 978-988-19251-5-2
ISSN: 2078-0958 (Print); ISSN: 2078-0966 (Online)